*Sensors and Materials*, Vol. 38, No. 10 (2026) 6289–6296
MYU Tokyo



S & M 4681

# Broadband Absorptance Retention of Black GaAs Nanotip Surfaces after Thermal Exposure for IR Sensor Interfaces

Yi-Fan Huang*

Department of Mechanical Engineering, National Chin-Yi University of Technology,
No. 57, Sec. 2, Zhongshan Rd., Taiping Dist., Taichung 411030, Taiwan (R.O.C.)

(Received August 6, 2026; accepted September 29, 2026)

***Keywords:*** black GaAs, broadband absorptance retention, thermal exposure, IR sensor interface

Broadband optical interfaces for IR sensing must retain stable spectral coupling after thermal exposure. In this study, p-type black GaAs nanotip arrays (GaAsNTs) fabricated by self-masked dry etching were evaluated at the materials level as front optical coupling interfaces for IR sensing. Hemispherical absorptance over 250–2400 nm was measured in the as-prepared state and after thermal exposure at 200, 500, and 700 °C for 30 min. All post-exposure spectra were acquired at room temperature after cooling, and NIR absorptance retention was used to quantify optical durability. The as-prepared GaAsNTs exhibited near unity broadband absorptance. After exposure at 200 and 500 °C, the response remained largely unchanged, with 98.5% NIR absorptance retention after 500 °C exposure. In contrast, exposure at 700 °C reduced retention to 75.8% and produced the cracking, nanotip collapse, and partial removal of the nanostructured layer, suggesting a structural contribution to optical degradation. To the best of our knowledge, this is the first systematic evaluation of broadband hemispherical absorptance retained by black GaAs nanotip surfaces after thermal exposure. These results provide an application-oriented materials assessment for IR sensor interface design under thermal exposure constraints. They also distinguish post-exposure durability from continuous high-temperature operation.

## 1. Introduction

IR sensing is widely used in thermal imaging, spectroscopic monitoring, environmental detection, and industrial process analysis.[1,2] Most IR photodetector studies emphasize carrier transport, dark current, responsivity, and signal readout.[3,4] However, the front optical interface also governs optical coupling into the sensor. In thermally demanding environments, post-exposure changes in absorptance, reflectance, or transmittance may cause signal loss, spectral variation, or baseline drift. Stable broadband coupling is therefore essential for reliable IR sensing under harsh thermal conditions.

GaAs is a direct band-gap semiconductor for IR sensing and optoelectronic applications, but its high refractive index causes substantial Fresnel reflection at the air and semiconductor

*Corresponding author: e-mail: yifanhuang@ncut.edu.tw
https://doi.org/10.18494/SAM6567

ISSN 0914-4935 © MYU K.K.
https://myukk.org/

interface.[3,5–7] Conventional antireflection coatings can reduce this loss through thin-film interference, although their performance depends on layer thickness, refractive index, incident angle, adhesion, and thermal expansion mismatch.[8,9] By comparison, nanostructured GaAs surfaces can regulate the effective refractive index distribution and optical propagation, thereby suppressing broadband reflection and enhancing absorption.[7,10–12] In our previous study, dense and aperiodic p-type GaAs nanotip arrays (GaAsNTs) exhibited near unity hemispherical absorptance over 250–2400 nm.[12] The above band-gap response was primarily associated with nanotip geometry and broadband optical coupling, whereas heavy doping contributed to below-band-gap NIR absorption. In that study, we established the fabrication, as-prepared morphology, and room-temperature broadband optical response of the GaAsNT surfaces, but did not evaluate their optical durability after thermal exposure.

The broadband optical response retained by black GaAs after thermal exposure remains insufficiently quantified. Studies of high-temperature absorbers and other black semiconductors have shown that high initial absorptance does not necessarily ensure post-exposure optical stability.[13,14] Previous microscopic studies examined thermally induced morphological evolution in individual GaAs nanowires and demonstrated the effects of diameter, crystal structure, and surface facets on decomposition behavior.[15,16] These studies provide nanoscale understanding but do not reveal whether thermal changes degrade the area-averaged broadband response of large-area black GaAs optical interfaces. To the best of our knowledge, the retained UV–VIS–NIR hemispherical absorptance of black GaAs surfaces after controlled thermal exposure has not yet been systematically evaluated.

In this study, p-type black GaAsNTs fabricated by self-masked dry etching (SMDE) were evaluated at the materials level as front optical coupling interfaces for IR sensing. In this context, the GaAsNT surface is intended to suppress front surface reflection and enhance broadband optical coupling into the GaAs material. The present study therefore is focused on the materials -level optical durability of this interface rather than the device level validation of a complete IR sensor. Hemispherical absorptance over 250–2400 nm was measured for as-prepared samples and after thermal exposure at 200, 500, and 700 °C for 30 min. All post-exposure spectra were acquired at room temperature after cooling. NIR absorptance retention was introduced as a normalized metric for post-exposure optical performance and compared with changes in surface appearance and morphology. The optical response remained largely preserved after exposure at 200 and 500 °C but degraded markedly after exposure at 700 °C. This work extends black GaAs research from initial optical performance to post-exposure durability and provides an application oriented experimental basis for evaluating its suitability as a broadband optical interface for IR sensing under thermal exposure constraints.

## 2. Materials

The p-type black GaAsNT surfaces were fabricated on one-side-polished (100) Zn-doped GaAs wafers by SMDE as reported previously.[12,17] The substrate carrier concentration was $0.5–5\times10^{19}$ $cm^{-3}$. Because the fabrication procedure, as-prepared morphology, and room-temperature optical properties were established previously,[12] the present work is focused on thermal exposure and post-exposure optical and morphological characterization. The as-

prepared state was used only as the reference for evaluating retained performance. The exposure temperatures of 200, 500, and 700 °C were selected as discrete conditions for comparative post-exposure evaluation, with a fixed duration of 30 min for direct comparison. These conditions were intended for materials-level screening rather than for reproducing specific IR sensor operating conditions. Thermal exposure was performed in a vacuum furnace evacuated to approximately $1 \times 10^{-4}$ Torr, followed by nitrogen introduction at 50 sccm to maintain approximately 0.2 Torr during exposure. After treatment, the samples were cooled naturally to room temperature inside the furnace. All subsequent optical measurements were therefore post-exposure measurements and were not performed in situ at the exposure temperatures.

Hemispherical optical properties were measured at room temperature using a UV–VIS–NIR spectrophotometer equipped with an integrating sphere (JASCO V-670, Tokyo, Japan). Hemispherical reflectance R and transmittance T were recorded from 250 to 2400 nm under normal incidence, and absorptance $A$ was calculated as $A\ (\%) = 100 - R\ (\%) - T\ (\%)$. All samples were measured to be approximately $1.0 \times 1.5$ cm$^2$ under identical conditions after cooling. The preservation of the NIR optical response was quantified using the NIR absorptance retention: NIR absorptance retention (%) = $(A_{NIR,post\ exposure} / A_{NIR,as\ prepared}) \times 100\%$.

Here, $A_{NIR,post\ exposure}$ and $A_{NIR,as\ prepared}$ are the average hemispherical absorptance values over 873–2400 nm after thermal exposure and in the as-prepared state, respectively. A value of 100% indicates the complete preservation of the average NIR absorptance. This normalized parameter enables the direct comparison of the NIR optical responses retained after different thermal exposures. Surface morphology was examined by field emission scanning electron microscopy (FE SEM, JEOL JSM 6700, Tokyo, Japan).

## 3. Results

Figure 1(a) shows the experimental framework extending our previous room-temperature characterization of black GaAsNT surfaces to post-exposure evaluation for IR sensor interfaces. The fabrication process, as-prepared nanotip morphology, and near-unity broadband hemispherical absorptance were established previously.[12,17] In the present study, these as-prepared characteristics serve only as the reference baseline, while the new analysis is focused on the optical and morphological responses retained after thermal exposure. The samples were exposed at 200, 500, and 700 °C for 30 min, cooled to room temperature, and then measured using a UV–VIS–NIR spectrophotometer. Because all spectra were acquired at room temperature under identical conditions, the observed differences represent optical changes retained after thermal exposure rather than in situ high-temperature behavior or continuous operating stability at the exposure temperatures. Accordingly, the three exposure temperatures were used as discrete comparative conditions and should not be interpreted as specific IR sensor operating temperatures.

Figure 1(b) shows the room-temperature hemispherical absorptance spectra of the planar p-type GaAs substrate and black GaAsNT surfaces in the as-prepared and thermally exposed states. The as-prepared GaAsNT surface exhibited a substantially higher broadband absorptance than the planar substrate, reaching 99.0, 99.1, and 93.2% at 300, 500, and 2000 nm, respectively (Table 1). After exposure at 200 and 500 °C for 30 min, the spectra remained close to the as-

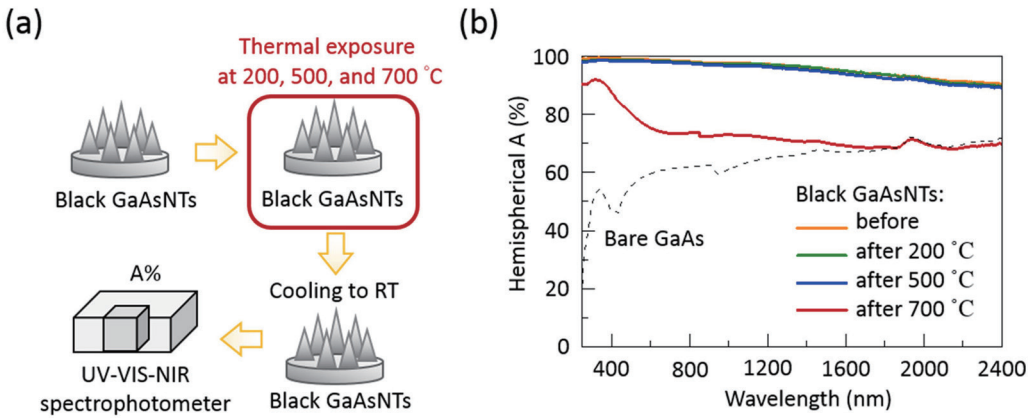



Fig. 1. (Color online) (a) Experimental workflow for thermal exposure and post-exposure optical measurements of p-type black GaAsNTs. (b) Room-temperature hemispherical absorptance spectra of planar GaAs and black GaAsNTs before and after exposure at 200, 500, and 700 °C for 30 min. All spectra were acquired at room temperature after cooling.

Table 1
Room-temperature hemispherical absorptance values of the planar p-type GaAs substrate and p-type black GaAsNT surfaces at selected wavelengths before and after thermal exposure.

| Sample | Condition | A% (300 nm) | A% (500 nm) | A% (2000 nm) |
|---|---|---|---|---|
| p-type GaAs | Substrate | 55.2 | 59.0 | 72.3 |
| p-type GaAsNTs | As-prepared | 99.0 | 99.1 | 93.2 |
| p-type GaAsNTs | 200 °C | 98.6 | 98.6 | 92.2 |
| p-type GaAsNTs | 500 °C | 98.4 | 98.4 | 91.6 |
| p-type GaAsNTs | 700 °C | 91.6 | 80.4 | 70.1 |

prepared response over 250–2400 nm, with decreases of only 0.4–1.6 percentage points at the selected wavelengths. In contrast, exposure at 700 °C reduced the absorptance to 91.6, 80.4, and 70.1%, respectively. The larger losses in the visible and NIR regions indicate the deterioration of the broadband optical coupling relevant to IR sensor interfaces. Thus, under the present 30 min exposure conditions, the optical response was largely preserved after exposure at 200 and 500 °C but degraded markedly at 700 °C.

Table 1 shows the absorptance values obtained at 300, 500, and 2000 nm, representing the UV, VIS, and NIR regions, respectively. The planar p-type GaAs substrate exhibited a substantially lower absorptance than the as-prepared nanotip surface. Changes after exposure at 200 and 500 °C were minor; after 500 °C exposure, the absorptance remained at 98.4, 98.4, and 91.6%. Exposure at 700 °C reduced these values to 91.6, 80.4, and 70.1%, respectively. At 2000 nm, the decrease was 23.1 percentage points, corresponding to a relative reduction of 24.8% and representing the largest loss among the selected wavelengths.

Table 2 shows the reported absorptance of black GaAs materials in the as-prepared and thermally exposed states above and below the GaAs band gap (Eg). At room temperature, the GaAs band gap of approximately 1.42 eV corresponds to an absorption edge near 873 nm.

Table 2
Black GaAs absorptance values in the as-prepared and thermally exposed states above and below the band gap (Eg). The corresponding ranges are 250–870 and 873–2400 nm, respectively, which are based on the room-temperature GaAs absorption edge near 873 nm.

| Wavelength range | As-prepared absorptance (%) | | Post-exposure absorptance (%) | | Reference |
|---|---|---|---|---|---|
| (nm) | Above Eg | Below Eg | Above Eg | Below Eg | |
| 240–2400 | 98–100 | 72-98 | - | - | 18 |
| 550–2600 | 90 | - | - | - | 19 |
| 400–700 | 98 | - | - | - | 20 |
| 375–750 | 98-99* | - | - | - | 21 |
| 375–1200 | 99.5* | 96.57* | - | - | 22 |
| 300–2000 | 99 | 33–60 | - | - | 7 |
| 300–2400 | 98–99 | 38 | - | - | 23 |
| 250–2400 | 98–99.7 | 92–98 | - | - | 12 |
| 250–2400 | 98–99.7 | 92–98 | 98–99 | 92–96 | This work |

Note: "*" denotes simulated values. "As-prepared" refers to samples before thermal exposure. For the present work, the listed post-exposure absorptance values correspond to exposure at 500 °C for 30 min and were measured at room temperature after cooling.

Accordingly, 250–870 and 873–2400 nm were defined as the above- and below-band-gap regions, respectively, while the narrow interval immediately adjacent to the absorption edge was excluded to avoid ambiguity in the transition region. Previous studies generally reported high above-Eg absorptance for black GaAs, whereas below-Eg absorptance was more variable and less frequently reported.[7,18–23] In our previous study, we established an as-prepared hemispherical absorptance of 98–99.7% above Eg and 92–98% below Eg over 250–2400 nm.[12] After exposure at 500 °C for 30 min, the absorptance remained at 98–99% above Eg and 92–96% below Eg, representing the highest post-exposure values among the studies listed. To the best of our knowledge, this is the first systematic broadband hemispherical absorptance assessment of black GaAs across both sides of the band gap after thermal exposure, supporting its evaluation as a thermally durable optical interface for IR sensing.

To relate the absorptance changes in Fig. 1(b) to surface evolution, the optical appearance and morphology were examined before and after thermal exposure. Figure 2(a) shows that bare GaAs changed from gray to dark black after GaAsNT formation, consistent with enhanced absorptance. The SEM image in Fig. 2(b) shows the dense and aperiodic nanotip morphology of the as-prepared surface, consistent with our previous characterization.[12] This morphology served as the structural reference for evaluating post-exposure degradation. After exposure at 700 °C for 30 min, the surface became brownish yellow [Fig. 2(c)], consistent with reduced visible absorptance. NIR degradation was evaluated from the spectra in Fig. 1(b) because it cannot be determined from surface appearance. The 200 and 500 °C samples are not shown because their spectra remained close to the as-prepared response and their surfaces remained dark.

Figure 2(d) shows a cracked boundary between GaAsNT-covered and partially removed regions. Higher magnification revealed collapsed and damaged nanotips with filament-like features [Fig. 2(e)], whereas little discernible GaAsNT coverage remained in the adjacent exposed region [Fig. 2(f)]. These observations indicate the spatially nonuniform degradation of the nanotip layer and are consistent with the broadband absorptance loss after exposure at 700 °C.

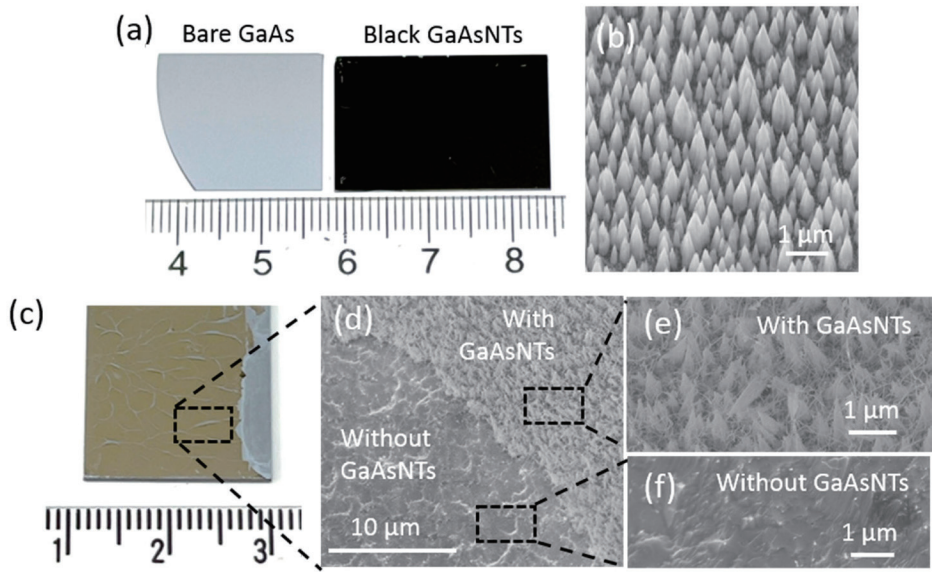



Fig. 2. (Color online) Optical and SEM images of p-type black GaAsNT surfaces (a),(b) in the as-prepared state and (c)–(f) after exposure at 700 °C for 30 min: (a),(c) optical appearance and (b),(d)–(f) surface morphology.

Figure 3 shows the NIR absorptance retention relative to that of the as-prepared state defined as 100%. The values were calculated from the average hemispherical absorptance over 873–2400 nm using room-temperature spectra acquired after cooling. The retention remained high after exposure at 200 and 500 °C, reaching 99.2 and 98.5%, respectively, but decreased to 75.8% after exposure at 700 °C. This reduction is consistent with the broadband absorptance loss in Fig. 1(b) and the structural degradation observed in Figs. 2(c)–2(f). The results indicate that NIR optical coupling relevant to IR sensor interfaces was largely retained after exposure at 200 and 500 °C but degraded markedly at 700 °C. Because intermediate temperatures were not examined, the transition remains unresolved between 500 and 700 °C. Therefore, 500 °C is the highest tested exposure temperature with largely preserved NIR performance, rather than a maximum operating temperature or continuous stability limit.

## 4. Discussion

In this study, the nanoscale thermal observations of individual GaAs nanowires are linked to the area-averaged optical response of large-area black GaAs surfaces.[15,16] Broadband hemispherical absorptance measurements after thermal exposure extend the evaluation from single nanostructures to the collective behavior of an optical interface. After exposure at 700 °C, the nanotip collapse, cracking, and partial removal of the nanostructured layer coincided with pronounced optical degradation. These structural changes may disrupt the gradual effective refractive index transition and optical propagation, suggesting a structural contribution to the absorptance loss. However, their quantitative contribution remains unresolved, and possible compositional or electronic changes cannot be excluded on the basis of the present data. The

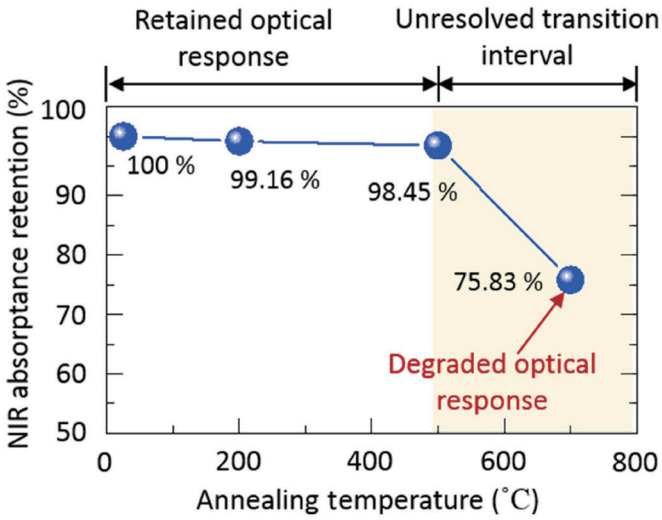



Fig. 3. (Color online) NIR absorptance retention of p-type GaAsNT surfaces after 30 min thermal exposure. The shaded region indicates the unresolved transition interval between 500 and 700 °C; the line is a guide for the eye.

post-exposure optical response measured at room temperature remained largely preserved after 30 min exposure at 200 and 500 °C but degraded markedly after exposure at 700 °C. Because intermediate temperatures were not examined, the transition between 500 and 700 °C remains unresolved, and 500 °C should be regarded only as the highest tested exposure temperature with preserved optical performance. These results provide preliminary materials-level guidance for thermal exposure conditions and protective optical interface design for IR sensing. However, absorptance retention reflects only the preservation of optical coupling at the material interface and does not directly establish detector responsivity, noise performance, detectivity, or overall sensor reliability. Furthermore, the present findings are limited to a single 30 min exposure under reduced-pressure nitrogen conditions and do not establish durability in air or oxidizing atmospheres, under repeated thermal cycling, or during continuous high-temperature operation. Further materials characterization and device-level evaluation are needed to relate structural evolution and absorptance retention to sensor performance.

## 5. Conclusions

In this study, the evaluation of black GaAs nanotip surfaces from as-prepared optical properties is extended to broadband response after thermal exposure. The post-exposure optical performance measured at room temperature was largely retained after 30 min exposure at 200 and 500 °C, whereas exposure at 700 °C resulted in pronounced absorptance loss and morphological degradation. These results provide an application-oriented materials-level basis for evaluating the suitability of black GaAs surfaces as front optical coupling interfaces for IR sensing under the tested thermal exposure conditions, rather than a validation of a complete IR sensor device.

## Acknowledgments

This work was supported by the Higher Education SPROUT Project of the Ministry of Education, Taiwan, under Grant No. GG15840501C04. The authors sincerely thank Dr. Kuei-Hsien Chen (Institute of Atomic and Molecular Sciences, Academia Sinica) and Prof. Li-Chyong Chen (Department of Physics and Center for Condensed Matter Sciences, National Taiwan University) for valuable discussions and access to research facilities.

## References

1 C. S. Prasad, H. O. Everitt, and G. V. Naik: Commun. Eng. **3** (2024) 172. https://doi.org/10.1038/s44172-024-00316-y
2 X. Tan, H. Zhang, J. Li, H. Wan, Q. Guo, H. Zhu, H. Liu, and F. Yi: Nat. Commun. **11** (2020) 5245. https://doi.org/10.1038/s41467-020-19085-1
3 T. Murata, S. Asahi, S. Sanguinetti, and T. Kita: Sci. Rep. **10** (2020) 11628. https://doi.org/10.1038/s41598-020-68461-w
4 X. Xue, M. Chen, Y. Luo, T. Qin, X. Tang, and Q. Hao: Light Sci. Appl. **12** (2023) 2. https://doi.org/10.1038/s41377-022-01014-0
5 D. E. Aspnes and A. A. Studna: Phys. Rev. B **27** (1983) 985. https://doi.org/10.1103/PhysRevB.27.985
6 B. Wang, E. Stevens, and P. W. Leu: Opt. Express **22** (2014) A386. https://doi.org/10.1364/OE.22.00A386
7 Y.-F. Huang, Y.-J. Jen, V. A. Modak, L.-C. Chen, and K.-H. Chen: Nanomaterials **14** (2024) 1154. https://doi.org/10.3390/nano14131154
8 T. Yang, X. Wang, W. Liu, Y. Shi, and F. Yang: Opt. Express **21** (2013) 18207. https://doi.org/10.1364/OE.21.018207
9 G. Womack, P. M. Kaminski, A. Abbas, K. Isbilir, R. Gottschalg, and J. M. Walls: J. Vac. Sci. Technol. A **35** (2017) 021201. https://doi.org/10.1116/1.4973909
10 R. Sanatinia, K. M. Awan, S. Naureen, N. Anttu, E. Ebraert, and S. Anand: Opt. Mater. Express **2** (2012) 1671. https://doi.org/10.1364/OME.2.001671
11 P. Lova, V. Robbiano, F. Cacialli, D. Comoretto, and C. Soci: ACS Appl. Mater. Interfaces **10** (2018) 33434. https://doi.org/10.1021/acsami.8b10370
12 Y.-F. Huang, W.-H. Lin, and J.-H. Chen: Mater. Lett. **416** (2026) 140687. https://doi.org/10.1016/j.matlet.2026.140687
13 Z. Wu, F. Chen, Z. Xuan, Y. Chen, W. Shi, X. Liu, and S. Wang: Opt. Mater. Express **10** (2020) 733. https://doi.org/10.1364/OME.384483
14 Y. Wang, J. Gao, H. Yang, X. Wang, and Z. Shen: Nanoscale Res. Lett. **11** (2016) 56. https://doi.org/10.1186/s11671-016-1281-4
15 I. Ilkiv, D. Kirilenko, K. Kotlyar, and A. Bouravleuv: Nanotechnology **31** (2020) 055701. https://doi.org/10.1088/1361-6528/ab4e27
16 P. Schmiedeke, F. Panciera, J.-C. Harmand, L. Travers, and G. Koblmüller: Nanoscale Adv. **5** (2023) 2994. https://doi.org/10.1039/D3NA00135K
17 C.-H. Hsu, H.-C. Lo, C.-F. Chen, C.-T. Wu, J.-S. Hwang, D. Das, J. Tsai, L.-C. Chen, and K.-H. Chen: Nano Lett. **4** (2004) 471. https://doi.org/10.1021/nl049925t
18 S. Ravipati, J. Shieh, F.-H. Ko, C.-C. Yu, H.-L. Chen, C.-T. Wu, and S.-H. Chen: Energy Environ. Sci. **5** (2012) 7601. https://doi.org/10.1039/C2EE21558F
19 Y. Song and J. Oh: Sol. Energy Mater. Sol. Cells **144** (2016) 159. https://doi.org/10.1016/j.solmat.2015.08.034
20 S. Behera, P. W. Fry, H. Francis, I. Farrer, C. Jin, and M. Hopkinson: AIP Adv. **10** (2020) 105211. https://doi.org/10.1063/5.0015404
21 R. Kumar, B. K. Singh, R. K. Tiwari, and P. C. Pandey: Opt. Quantum Electron. **54** (2022) 416. https://doi.org/10.1007/s11082-022-03798-2
22 R. Kumar, B. K. Singh, and P. C. Pandey: Bull. Mater. Sci. **46** (2023) 164. https://doi.org/10.1007/s12034-023-02999-z
23 Y.-F. Huang, V. A. Modak, C.-Y. Huang, L.-C. Chen, and K.-H. Chen: Mater. Sci. Semicond. Process. **186** (2025) 109117. https://doi.org/10.1016/j.mssp.2024.109117